Inorganic Chemistry

Article

pubs.acs.org/IC

Metal Ion Complexes of *N,N′*-Bis(2-Pyridylmethyl)-1,3-Diaminopropane-*N,N′*-Diacetic Acid, H_2bppd

Daniel S. Kissel,[†] Jan Florián,[†] Craig C. McLauchlan,[‡] and Albert W. Herlinger*[,†]

[†]Department of Chemistry and Biochemistry, Loyola University Chicago, 1032 West Sheridan Road, Chicago, Illinois, 60660 United States

[‡]Department of Chemistry, Illinois State University, Campus Box 4160, Normal, Illinois 61790-4160, United States

Supporting Information

ABSTRACT: A higher yield synthesis of *N,N′*-bis(2-pyridylmethyl)-1,3-diaminopropane-*N,N′*-diacetic acid (H_2bppd) and its complexation of trivalent metal ions (Al(III), Ga(III), In(III)) and selected lanthanides (Ln(III)) are reported. H_2bppd and the metal−bppd^{2-} complexes, isolated as hexafluorophosphate salts, were characterized by elemental analysis, mass spectrometry, IR, and ^{1}H and ^{13}C NMR spectroscopy. [Ga(bppd)]PF_6, [Ga($C_{19}H_{22}N_4O_4$)]PF_6, was crystallized as colorless needles by slow evaporation from anhydrous methanol; its molecular structure was solved by direct X-ray crystallography methods. The compound crystallized in the monoclinic space group $P2_1/c$, with a = 9.6134(2) Å, b = 20.2505(4) Å, c = 11.6483(3) Å, β = 97.520(1)°, and Z = 4. Ga is coordinated in a distorted octahedral geometry provided by a N_4O_2 donor atom set with cis-monodentate acetate groups and *cis*-2-pyridylmethyl N atoms. Quantum mechanical calculations were performed for the three possible geometric isomers of a pseudo-octahedral metal−bppd^{2-} complex with five different metal ions. The results indicate, that in aqueous solution, the stability of the *trans*-O,O isomer is similar to that of the *cis*-O,O; *cis*-N_{py},N_{py} isomer but is greater than that of the *trans*-N_{py},N_{py} isomer. Calculations for a six-coordinate La(III)-bppd^{2-} complex converge to a structure with a very large N_{py}−La−N_{py} bond angle (146.4°), a high metal charge (2.28 au), and a high solvation free energy (−79.4 kcal/mol). The most stable geometric arrangement for bppd^{2-} around the larger La(III) is best described as an open nestlike structure with space available for additional ligands. IR spectroscopy was used to investigate the nature of the H_2bppd−metal complexes isolated in the solid state and the binding modes of the carboxylate functionalities. The spectra indicate that fully deprotonated [M(bppd)]$^+$ complexes as well as partially protonated complexes [M(Hbppd)Cl]$^+$ were isolated. The ^{1}H and ^{13}C assignments for H_2bppd and metal−bppd^{2-} complexes were made on the basis of 2D COSY, NOESY, and ^{1}H−^{13}C HSQC experiments, which were used to differentiate among the cis (C_1 symmetry) and the two trans (C_2 symmetry) isomers.

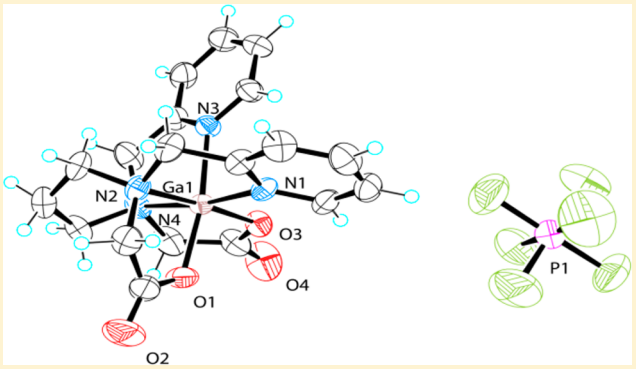

INTRODUCTION

The interaction of polyaminocarboxylate ligands with f-element metal ions is an active area of research.[1] Polyaminocarboxylic acids find use in the TALSPEAK process, which employs DTPA, diethylenetriaminepentaacetic acid, as an effective hold back reagent for lanthanide(III)−actinide(III) separation; however, DTPA's efficacy requires high lactic acid concentrations to prevent precipitation and improve extraction kinetics.[2] Derivatives of polyaminocarboxylic acids are also of interest as potential solvent extraction reagents for spent nuclear fuel reprocessing, as magnetic resonance imaging agents when coordinated to lanthanides, and in nuclear medicine when coordinated to radioactive Group 13 nuclides.[3−7]

N,N′-Bis(2-pyridylmethyl)-1,3-diaminopropane-*N,N′*-diacetic acid, H_2bppd, is a symmetrically disubstituted diaminocarboxylic acid with a propylene backbone. Our interest in H_2bppd resides in its potential for use as a complexation reagent for trivalent lanthanide−actinide (Ln(III)−An(III)) separations. This chemical separation is one of the more difficult challenges in spent nuclear fuel reprocessing because of the very similar physiochemical properties of Ln(III) and An(III) ions. It has been shown that donor atoms softer than oxygen make this difficult separation more selective but at the cost of complex stability.[8,9] Polyaminocarboxylic acids, containing softer aromatic nitrogen donors and harder oxygen donors, have been shown to provide good metal ion selectivity with adequate complex stability.[6] The H_2bppd molecule contains softer 2-pyridylmethyl substituents to provide selectivity and harder acetate functionalities to improve stability. The propylene chain of the diamine backbone provides flexibility and the ability to form a 6-membered

Received: November 12, 2013
Published: March 21, 2014

chelate ring. Hancock has suggested a rule for ligand design that an "increase of chelate ring size from five membered to six membered in a complex will increase the stability of smaller relative to larger metal ions".[10,11] Indeed, the increase in complex stability for polyamine ligands containing pyridyl and saturated nitrogen atoms as donor groups that was observed upon changing chelate size from five- to six-membered rings supports this rule.[12] Further, it has been suggested that this strategy could be employed in designing ligands that show size selectivity for Al(III).[13]

H_2bppd was previously prepared as part of a study of vanadium(III) coordination stereochemistry with hexadentate ligands.[14] In the present study, H_2bppd was synthesized by a facile, two-step procedure using simple starting materials that employs bromoacetic acid, a strong alkylating agent, to provide higher yields. Syntheses for the related *N,N′*-bis(2-pyridylmethyl)-1,2-diaminoethane-*N,N′*-diacetic acid, H_2bped, by alternative routes have been reported.[3,15]

Very little structural information is available for H_2bppd and its metal complexes because of the difficulty in obtaining crystals suitable for X-ray crystallographic analysis. As has been previously noted, this difficulty likely arises from the flexibility of the ligand species and the many geometric and coordination isomers that are possible when a metal−ligand complex forms.[4,16,17] A structure is available for a bridged dinuclear vanadium complex of a derivative of H_2bppd, which has a hydroxyl substituent in the 2-position of the propylene unit.[18,19] There are three structural reports of the related cobalt(III)-*N,N′*-bis(2-pyridylmethyl)-1,2-diaminoethane-*N,N′*-diacetato complex $[Co(bped)]^+$ with different counterions, that is, ClO_4^-, BF_4^-, and PF_6^-,[3,16,17] and an ethyl ester version of the $bped^{2-}$ ligand with Mn(II).[20] We previously reported a structure for the cobalt(III)-$bppd^{2-}$ compound $[Co(bppd)]PF_6$.[21] The Co(III)−$bppd^{2-}$ and Co(III)−$bped^{2-}$ complexes have the acetate O atoms in a trans orientation. In the $[Ga(bppd)]PF_6$ structure reported here, the acetate O atoms are cis with respect to each other. A third possible $[M(bppd)]^+$ isomer with *trans*-N_{py},N_{py} pyridine groups has not been observed for any metal ion, Figure 1.

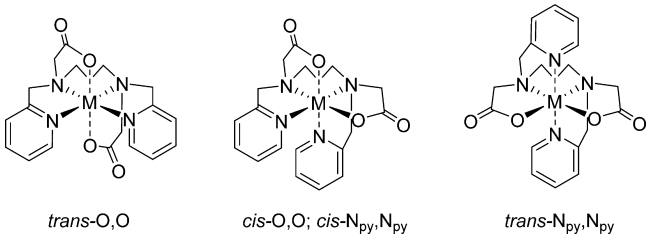

Figure 1. Coordination geometry for *trans*-O,O $[Co(bppd)]^+$ and *cis*-O,O; *cis*-N_{py},N_{py} $[Ga(bppd)]^+$. The third possible geometric isomer, *trans*-N_{py},N_{py} $[M(bppd)]^+$, has not yet been structurally characterized.

The present investigation is devoted to exploring correlations between the spectral features of $[M(bppd)]^+$ complexes and their structure to establish criteria that differentiate among different types of carboxylate bonding and cis and trans geometric isomers. Correlations of this type become particularly useful for compounds where no X-ray data are available. Although several groups, particularly Caravan and co-workers,[3,4] have directed considerable effort at X-ray structural characterization of 2-pyridylmethyl-substituted polyaminocarboxylate complexes, it is clear that the time and effort involved in these studies makes development of efficient alternative determinative techniques desirable. Further, to gain insight into the complexation process, the energies of the three possible geometric isomers for pseudo-octahedral trivalent metal complexes, $[M(bpad)]^+$, relative to the *trans*-O,O isomer, have been obtained by quantum mechanical calculations for diamines with different alkyl chains (*a*) and six trivalent metal ions.

EXPERIMENTAL SECTION

Reagents. Reagent grade aluminum chloride hexahydrate, cobalt chloride hexahydrate, dysprosium nitrate hexahydrate, lanthanum nitrate hexahydrate, neodymium nitrate hexahydrate, samarium nitrate hexahydrate, indium nitrate hydrate, and gallium nitrate hydrate obtained from Fisher Scientific, were used as received. Reagent grade sodium hexafluorophosphate, potassium hydrogen phthalate (KHP), 1,2-diaminoethane, 1,3-diaminopropane, anyhydrous methanol, 2-pyridinecarboxaldyde, bromoacetic acid, 30% by weight hydrogen peroxide, chloroform-*d* ($CDCl_3$), sodium borohydride, and deuterium oxide (D_2O), obtained from Sigma Aldrich Chemical Co., were used without further purification. $[Co(bppd)]PF_6$ was prepared as previously reported.[21] Dowex 50W-X8 (100−200 mesh) cation exchange resin was obtained from Fischer Scientific and prepared by washing with a solution of 30% by weight H_2O_2 (33 mL) in 1.79 M NaOH (67 mL) followed by a second wash with copious amounts of deionized water. The resin was swollen in the column by eluting with 6 M HCl and washed again with copious amounts of deionized water.

Methods. Combustion analyses were done by Galbraith Laboratories, Inc., Knoxville, TN using GLI Procedure ME-14. Equivalent weight titrations with 0.02 M NaOH, standardized against KHP, were conducted in a 50 mL glass flow through cell using phenolphthalein as the indicator. ^{1}H and ^{13}C NMR spectra referenced to internal TMS for $CDCl_3$ solutions were recorded on a Varian Unity INOVA 500 MHz spectrometer; for labeling see Figure 2. ^{1}H and ^{13}C NMR spectra

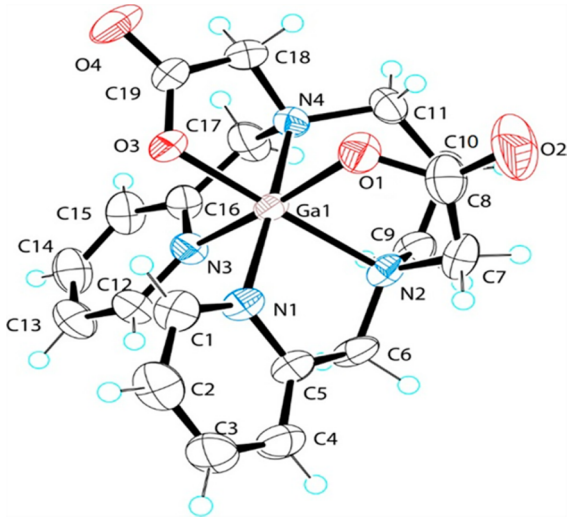

Figure 2. Thermal displacement plot (50%) of the $[Ga(bppd)]^+$ cation. H atoms are shown as circles of arbitrary size.

recorded for samples in D_2O were referenced to residual solvent[22] and external DSS, respectively. The ^{1}H COSY and ^{1}H NOESY correlation spectra were recorded on a Varian Inova 500 MHz spectrometer. The ^{1}H−^{13}C-detected heteronuclear single-quantum coherence (HSQC) experiments were performed on a Aglient DD2 500 MHz spectrometer. Mass spectra were obtained with an Agilent 6460 Triple Quad LC/MS instrument in full scan mode by direct infusion using an aqueous 70% by mass ethanol solution. Intensity data for solving the $[Ga(bppd)]PF_6$ structure were collected on a Bruker SMART Apex 2 diffractometer. Infrared spectra were obtained on a

dx.doi.org/10.1021/ic402810e | Inorg. Chem. 2014, 53, 3404−3416

Thermo Nicolet Nexus 470 FTIR spectrometer calibrated in the 4000−400 cm^{-1} spectral range using polystyrene. Samples were prepared as KBr pellets and run with air as the background. The spectra were checked as nujol and/or fluorolube mulls. Routine spectra were recorded collecting 32 scans at 4 cm^{-1} resolution.

Synthesis of Ligands. The syntheses of the 2-pyridylmethyl-substituted diamines and their subsequent elaboration to the diacetic acids were achieved using the same procedures that are given here in detail only for the 1,3-diaminopropane derivatives.

***Caution**: Bromoacetic acid is a very reactive and toxic, strong alkylating agent that should be used in a hood while wearing gloves.*

***N,N′*-Bis(2-pyridylmethyl)-1,3-diaminopropane, bpmdap.** A solution of 1,3-diaminopropane (1.12 g, 15.0 mmol) in anhydrous methanol (25 mL) was allowed to stir under a N_2 atmosphere in the presence of freshly activated 3 Å molecular sieves (5.0 g) for 15 min. A solution of 2-pyridinecarboxaldehyde (3.25 g, 30.0 mmol) in anhydrous methanol (25 mL) was then slowly added dropwise with continuous stirring. After the addition was complete, the reaction was refluxed for 3 h, and the resulting yellow-orange mixture was filtered to remove the molecular sieves. The filtrate was returned to the original reaction vessel, cooled to 0 °C, and solid $NaBH_4$ (1.32 g, 35.0 mmol) slowly added with efficient stirring. The reaction mixture was warmed to room temperature and refluxed for an additional 2 h. After the reaction mixture cooled to room temperature, a solution of NaOH (5.0 g in 17 mL H_2O) was added and the resulting red-orange solution was extracted with methylene chloride (4 × 20 mL portions). The CH_2Cl_2 was dried over anhydrous potassium carbonate, filtered, and the diamine product isolated as a viscous oil by evaporation under reduced pressure at 60 °C. Yield: 4.10 g (13.7 mmol, 91%). ^{1}H NMR (ppm, $CDCl_3$): 1.59 (p, 2H, NHCH$_2$*CH*$_2$CH$_2$NH, J = 7.6 Hz), 2.42 (t, 4H, NH*CH*$_2$CH$_2$*CH*$_2$NH, J = 7.5 Hz), 3.66 (s, 4H, NH*CH*$_2$py), 7.19 (t, 2H, NCCHCH*CH*CH, J = 6.8 Hz), 7.25 (d, 2H, NC*CH*CHCHCH, J = 8.5 Hz), 7.68 (t, 2H, NCCH*CH*CHCH, J = 8.0 Hz, 1.5 Hz), and 8.32 (d, 2H, NCCHCHCH*CH*, J = 5.2 Hz).

***N,N′*-Bis(2-pyridylmethyl)-1,2-diaminoethane, bpmdae.** Yield: 3.53 g (14.7 mmol, 98%). ^{1}H NMR (ppm, $CDCl_3$): 2.83 (s, 4H, NH*CH*$_2$*CH*$_2$NH), 3.92 (s, 4H, NH*CH*$_2$py), 7.14 (td, 2H, NCCHCH*CH*CH, J = 6.2 Hz, 0.6 Hz), 7.30 (d, 2H, NC*CH*CHCHCH, J = 7.8 Hz), 7.62 (td, 2H, NCCH*CH*CHCH, J = 7.7 Hz, 1.9 Hz), and 8.54 (d, 2H, NCCHCHCH*CH*, J = 4.8 Hz).

***N,N′*-Bis(2-pyridylmethyl)-1,3-diaminopropane-*N,N′*-diacetic acid trihydrochloride, H_2bppd·3HCl.** A solution of bpmdap (3.48 g, 13.7 mmol) in 40 mL of cold deionized water was placed in an ice bath and stirred under N_2 for 15 min. A solution of bromoacetic acid (4.17 g, 30.0 mmol, in 9.0 mL of H_2O) was neutralized with NaOH (1.20 g in 17 mL of H_2O, 30.0 mmol) and slowly added dropwise to the cold bpmdap solution. After the addition was complete, a second aliquot of NaOH (1.10 g in 15 mL of H_2O, 27.4 mmol) was added to the yellow-brown reaction mixture and stirred overnight at room temperature. The strongly basic reaction mixture was extracted with methylene chloride, CH_2Cl_2, (4 × 20 mL portions) to remove unreacted amine and neutral organic impurities. The crude product was isolated from the aqueous phase by evaporation under reduced pressure at 60 °C. The isolated solid was dissolved in a minimal amount of deionized water, loaded onto a Dowex 50W-X8 cation exchange column (10 g, 20 mm × 38 cm, resin height 12 cm), and washed with 3 column volumes of water followed by 6 column volumes of 1.0 M HCl to remove Na^+ ions. The pure H_2bppd product was eluted as the trihydrochloride salt using 6 column volumes of 3.0 M HCl. (H_2bppd elutes more rapidly at higher HCl concentrations, but a lower purity product may be obtained.) The diacetic acid was obtained as a white, hygroscopic solid by evaporation of the 3.0 M HCl eluent under reduced pressure at 60 °C and dried in vacuo overnight at 60 °C. Yield: 4.40 g (8.22 mmol, 60%). The bulk material was obtained as a trihydrate. Anal. obs. (calcd) for $C_{19}H_{24}N_4O_4$·3HCl·3H_2O: C, 42.07 (42.59); H, 5.77 (6.20); N, 9.99 (10.45). IR (ν(cm^{-1})), fluorolube): 3356−2495 (s, b, O−H, N−H$^+$ str), 1727 (s, C═O str), 1609 (m, O−H, N−H$^+$ def), 1549 (m, py str), 1524 (m, py str), 1461 (m, CH_2 def), 1404 (m, C−O str). Equiv. Wt: obs. 103 g/eq$_{\cdot H+}$; calcd 107 g/eq$_{\cdot H+}$.

***N,N′*-Bis(2-pyridylmethyl)-1,2-diaminoethane-*N,N′*-diacetic Acid Tetrahydrochloride, H_2bped·4HCl.** Yield: 5.30 g (11.4 mmol, 77%). Anal. obs. (calcd) for $C_{18}H_{22}N_4O_4$·4HCl·H_2O: C, 40.85 (41.40); H, 5.06 (5.40); N, 10.52 (10.73). ^{1}H NMR (ppm, D_2O): 3.41 (s, 4H, NC*H*$_2$*CH*$_2$N), 3.73 (s, 4H, NCH$_2$py), 4.49 (s, 4H, NC*H*$_2$COOH), 7.83 (td, 2H, NCCHCH*CH*CH, J = 6.9 Hz, 0.6 Hz), 7.92 (d, 2H, NC*CH*CHCHCH, J = 7.5 Hz), 8.35 (td, 2H, NCCH*CH*CHCH, J = 7.9 Hz, 1.8 Hz), and 8.66 (d, 2H, NCCHCHCH*CH*, J = 5.7 Hz). IR (ν(cm^{-1})), fluorolube): 3384−2495 (s, b, O−H, N−H$^+$ str), 1727 (s, C═O str), 1609 (m, O−H, N−H$^+$ def), 1542 (m, py str), 1524 (m, py str), 1461 (m, CH_2 def), 1405 (m, C−O str). Equiv. Wt: obs. 89 g/eq$_{\cdot H+}$; calcd 87 g/eq$_{\cdot H+}$.

Synthesis of Metal Complexes. The synthetic procedures for the Group 13 metal complexes, [M(bppd)]PF_6 and [M(Hbppd)Cl]PF_6 were similar in all cases. One representative synthesis is given for each unique procedure. The Ln[bppd]PF_6 compounds were prepare at room temperature in a similar manner, but the chloride salts were used for the lighter lanthanides, La(III) and Nd(III), to avoid inclusion of inorganic salts.[4]

Na_2bppd. H_2bppd·3HCl·3H_2O (48 mg, 0.10 mmol) was dissolved in 5.0 mL of deionized water and neutralized with NaOH (18 mg in 237 μL of H_2O, 0.45 mmol). The solution was allowed to stir for 30 min and a white solid was collected by evaporation at 60 °C under reduced pressure. Yield: 35 mg, (0.090 mmol, 90%). IR (ν(cm^{-1})), fluorolube): 3080 (s, b, O−H str), 3030 (m, C−H aryl str), 2934 (m, CH_2 str), 2807 (m, CH_2 str), 1588 (s, COO^- str), 1474 (w, py str), 1433 (m, CH_2 def), 1405 (s, COO^- str).

[Al(bppd)]PF_6. A solution of $AlCl_3$·6H_2O (84 mg, 0.34 mmol) in anhydrous methanol (25 mL) was added dropwise with efficient stirring to a solution of H_2bppd·3HCl·3H_2O (180 mg, 0.34 mmol) in anhydrous methanol (25 mL) under a N_2 atmosphere. After the addition was complete, sodium acetate (139 mg, 1.70 mmol) was added as a dry solid to the colorless solution. The reaction was refluxed for 30 min and allowed to cool to room temperature. The solution was filtered; sodium hexafluorophosphate (59 mg, 0.35 mmol) was added to the reaction mixture, and the mixture was allowed to stir for 15 min. The reaction mixture was filtered and allow to stand overnight at room temperature. The crude product that formed was collected by suction filtration, dissolved in a minimal amount of hot methanol (~15 mL), and stirred for 15 min. The mixture was filtered warm, and the filtrate was collected in a 50 mL beaker. A white solid precipitated from the filtrate upon standing overnight. The solid was washed with cold methanol (3 × 5.0 mL), acetone (3 × 5.0 mL), and dried in vacuo overnight at 65 °C. Yield 140 mg (0.26 mmol, 77%). MS (+ESI): m/z 397.2 ([^{27}Al]$^+$, [$AlC_{19}H_{22}N_4O_4$]$^+$). IR (ν(cm^{-1}), KBr): 3057 (m, b, C−H aryl str), 2955 (m, b, CH_2 str), 2850 (m, b, CH_2 str), 1670 (s, b, COO^- str), 1617 (s, py str), 1577 (w, py str), 1466 (m, CH_2 def), 1442 (m, CH_2 def), 1385 (m, COO^-).

[Ga(bppd)]PF_6. After bulk synthesis as above, crystals suitable for X-ray diffraction studies were obtained by slow evaporation of a methanol solution at 16 °C. The colorless needles were collected and washed with cold methanol and acetone (3 × 2.0 mL portions each). Analyses were conducted on the crystalline material used in the X-ray diffraction studies. Yield: 120 mg (0.20 mmol, 60%). Anal. obs. (calcd) for $GaC_{19}H_{22}N_4O_4PF_6$: C, 39.00 (38.82); H, 3.79 (3.89); N, 9.58 (9.18). MS (+ESI): m/z 439.2 and 441.2 ([^{69}Ga]$^+$ and [^{71}Ga]$^+$, [$GaC_{19}H_{22}N_4O_4$]$^+$). IR (ν(cm^{-1}), KBr): 3124 (m, b, C−H aryl str), 3074 (m, b, C−H aryl str), 3044 (m, b, C−H aryl str), 2984 (m, b, CH_2 str), 2956 (m, b, CH_2 str), 2903 (m, b, CH_2 str), 1683 (vs, COO^- str), 1610 (m, py str), 1574 (w, py str), 1492 (w, py str), 1475 (m, py str), 1451 (m, CH_2 def), 1437 (m, CH_2 def), 1348 (s, COO^- str).

[In(bppd)]PF_6. Yield: 55 mg (0.10 mmol, 29%). Anal. obs. (calcd) for $InC_{19}H_{22}N_4O_4PF_6$: C, 36.12 (36.21); H, 4.12 (3.52); N, 8.56 (8.89). MS (+ESI): m/z 485.2 ([^{115}In]$^+$, [$InC_{19}H_{22}N_4O_4$]$^+$). IR (ν(cm^{-1}), KBr): 3063 (m, C−H aryl str), 2925 (m, CH_2 str), 2854 (m, CH_2 str), 1644 (vs, COO^- str), 1607 (s, py str), 1485 (w, py str), 1444 (m, CH_2 def), 1384 (s, COO^- str).

dx.doi.org/10.1021/ic402810e | *Inorg. Chem.* 2014, 53, 3404−3416

[Al(Hbppd)Cl]PF_6. A solution of H_2bppd·3HCl·3H_2O (270 mg, 0.50 mmol) in anhydrous methanol (25 mL), neutralized with 3 equivalents of sodium acetate (120 mg, 1.5 mmol), was added dropwise to a stirred solution of $AlCl_3$·6H_2O (120 mg, 0.50 mmol) in anhydrous methanol (20 mL) under a N_2 atmosphere. The reaction mixture was heated to reflux and solid sodium hexafluorophosphate (59 mg, 0.35 mmol) slowly added after the heating was stopped. The reaction mixture was stirred for 20 min and filtered hot. The filtrate was collected, cooled, and [Al(Hbped)Cl]PF_6 formed as a white solid upon standing overnight at room temperature. The product was collected by suction filtration, washed with cold methanol (2 × 5.0 mL portions) and ether (2 × 5.0 mL portions) and dried in vacuo overnight at 65 °C. Yield 61 mg (0.11 mmol, 22%). MS (+ESI): m/z 433.2 and 435.2 ([^{27}Al and ^{35}Cl]$^+$ and [^{27}Al and ^{37}Cl]$^+$, [$AlC_{19}H_{23}N_4O_4Cl$]$^+$). IR (ν(cm^{-1}), fluorolube): 3230 (s, b, O−H str), 3067 (s, C−H aryl str), 3007 (s, CH_2 str), 2957 (s, CH_2 str), 1735 (m, C═O str), 1636 (s, COO^- str), 1618 (s, py str), 1546 (w, py str), 1395 (s, COO^-).

[Ga(Hbppd)Cl]PF_6. Yield: 54 mg (0.13 mmol, 26%). MS (+ESI): m/z 475.2 and 477.2 ([^{69}Ga and ^{35}Cl]$^+$ and [^{71}Ga and ^{35}Cl]$^+$, [$GaC_{19}H_{23}N_4O_4Cl$]$^+$). IR (ν(cm^{-1}), KBr): 3434 (s, b, O−H str), 2961 (m, CH_2 str), 1734 (s, C═O str), 1653 (vs, COO^- str), 1616 (s, py str), 1577 (w, py str), 1488 (w, py str), 1448 (m, CH_2 def), 1384 (s, COO^-).

[In(Hbppd)Cl]PF_6. Yield: 170 mg (0.29 mmol, 58%). MS (+ESI): m/z 521.1 and 523.1 ([^{115}In and ^{35}Cl]$^+$ and [^{115}In and ^{37}Cl]$^+$, [$InC_{19}H_{23}N_4O_4Cl$]$^+$). IR (ν(cm^{-1}), KBr): 3486 (s, b, O−H str), 3067 (m, C−H aryl str), 2952 (m, CH_2 str), 1731 (s, C═O str), 1608 (vs, COO^- str), 1542 (m, py str), 1484 (w, py str), 1445 (s, CH_2 def), 1384 (s, COO^-).

[La(bppd)]PF_6·2H_2O. Yield: 120 mg (0.18 mmol, 53%). Anal. obs. (calcd) for $LaC_{19}H_{22}N_4O_4PF_6$·2H_2O: C, 32.85 (33.05); H, 3.42 (3.79); N, 8.36 (8.12). MS (+ESI): m/z 509.2 ([^{139}La]$^+$, [$LaC_{19}H_{22}N_4O_4$]$^+$). IR (ν(cm^{-1}), fluorolube): 3382 (m, b, O−H str), 3060 (m, C−H aryl str), 2963 (m, CH_2 str), 2855 (m, CH_2 str), 1601 (vs, b, COO^- str), 1443 (s, CH_2 def), 1413 (s, COO^- str).

[Nd(bppd)]PF_6·3H_2O. Yield: 220 mg (0.30 mmol, 88%). Anal. obs. (calcd) for $NdC_{19}H_{22}N_4O_4PF_6$·3H_2O: C, 31.75 (31.97); H, 3.89 (3.95); N, 8.12 (7.86). MS (+ESI): m/z 512.2 ([^{141}Nd]$^+$, [$NdC_{19}H_{22}N_4O_4$]$^+$). ^{1}H NMR (ppm, D_2O): 2.00 (s, 2H, $NCH_2CH_2CH_2N$), 3.16 (s, 4H, $NCH_2CH_2CH_2N$), 3.98 (s, 4H, NCH_2COO), 4.41 (s, 4H, NCH_2py), 7.60 (s, 4H, NCCHCHCHCH and NCCHCHCHCH), 7.99 (s, 2H, NCCHCHCHCH), and 8.85 (s, vb, 2H, NCCHCHCHCH). ^{13}C NMR (ppm, D_2O): 22.98, C(10); 51.78, C(9); 54.79, C(7); 61.05, C(6); 128.22, C(4); 128.55, C(2); 142.50, C(3); 151.26, C(1); 152.09, C(5); 173.08, C(8). IR (ν(cm^{-1}), fluorolube): 3381 (m, b, O−H str), 3063 (m, C−H aryl str), 2961 (m, CH_2 str), 2850 (m, CH_2 str), 1603 (vs, b, COO^- str), 1487 (m, py str), 1444 (s, CH_2 def), 1414 (s, COO^-str).

[Sm(bppd)]PF_6·3H_2O. Yield: 200 mg (0.28 mmol, 82%). Anal. obs. (calcd) for $SmC_{19}H_{22}N_4O_4PF_6$·3H_2O: C, 31.19 (31.70); H, 3.74 (3.92); N, 7.99 (7.78). MS (+ESI): m/z 522.2 ([^{152}Sm]$^+$, [$SmC_{19}H_{22}N_4O_4$]$^+$). ^{1}H NMR (ppm, D_2O): 2.18 (s, 2H, $NCH_2CH_2CH_2N$), 3.27 (s, 4H, $NCH_2CH_2CH_2N$), 3.78 (s, 4H, NCH_2COO), 4.50 (s, 4H, NCH_2py), 7.57 (s, 4H, NCCHCHCHCH and NCCHCHCHCH), 8.01 (s, 2H, NCCHCHCHCH), and 8.67 (s, 2H, NCCHCHCHCH). ^{13}C NMR (ppm, D_2O): 22.83, C(10); 55.02, C(9); 59.06, C(7); 60.99, C(6); 127.87, C(4); 128.21, C(2); 142.51, C(3); 151.17, C(1); 152.19, C(5); 173.95, C(8). IR (ν(cm^{-1}), fluorolube): 3392 (m, b, O−H str), 3030 (m, C−H aryl str), 2961 (m, CH_2 str), 2855 (m, CH_2 str), 1603 (vs, b, COO^- str), 1487 (m, py str), 1444 (s, CH_2 def), 1414 (s, COO^- str).

[Dy(bppd)]PF_6·2H_2O. Yield: 240 mg (0.33 mmol, 97%). Anal. obs. (calcd) for $DyC_{19}H_{22}N_4O_4PF_6$·2H_2O: C, 31.64 (31.96); H, 3.68 (3.67); N, 8.21 (7.85). MS (+ESI): m/z 534.2 ([^{164}Dy]$^+$, [$DyC_{19}H_{22}N_4O_4$]$^+$). IR (ν(cm^{-1}), fluorolube): 3392 (m, b, O−H str), 2930 (m, CH_2 str), 2850 (m, CH_2 str), 1605 (vs, b, COO^- str), 1487 (m, py str), 1446 (s, CH_2 def), 1414 (s, COO^- str).

[Co(bpmdap)Cl_2]PF_6·2H_2O. A methanol solution of bpmdap (120 mg in 8.0 mL, 0.46 mmol) was added dropwise to a stirred solution of $CoCl_2$·6H_2O (120 mg, 0.50 mmol) in anhydrous methanol (8.0 mL). The dark brown reaction mixture was aerated in the presence of activated charcoal and allowed to stir overnight at room temperature. The resulting reddish brown solution was filtered and sodium hexafluorophosphate (84 mg, 0.50 mmol) added to the filtrate with stirring. A red-brown solid precipitated from solution upon standing at room temperature for 48 h. The isolated solid was collected by suction filtration, washed with cold methanol (3 × 5.0 mL portions), and dried overnight at 75 °C. Yield: 110 mg (0.20 mmol, 43%). Anal. obs. (calcd) for $CoC_{15}H_{18}N_4Cl_2PF_6$·2$H_2O$: C, 31.76 (31.88); H, 3.65 (3.21). IR (ν(cm^{-1}), KBr): 3439 (s, b, O−H, N−H str), 3100 (m, C−H aryl str), 2925 (m, CH_2 str), 2855 (m, CH_2 str), 1612 (s, py str), 1483 (m, py str), 1447 (s, CH_2 def), 1424 (m, CH_2 def), 1294 (m), 841 (vs, N−H def), 558 (m).

X-ray Crystallography. Intensity data were collected for single crystals of [Ga(bppd)]PF_6 at 23 °C on a Bruker SMART Apex 2 diffractometer equipped with a CCD area detector using graphite monochromated Mo Kα radiation. Data were reduced and corrected for absorption using the SAINT+ Software Suite.[23] Structure solutions were obtained by direct methods and were refined on F^2 with the use of full-matrix least-squares techniques.[24] All non-hydrogen atoms were refined anisotropically and hydrogen atoms were refined with a riding model. Selected crystallographic details are shown in Table 1. More extensive crystallographic details are included in the Supporting Information, Figure S1.

Table 1. Crystallographic Parameters for [Ga(bppd)]PF_6

empirical formula	$C_{19}H_{22}F_6GaN_4O_4P$
moiety formula	$C_{19}H_{22}GaN_4O_4$, PF_6
formula weight	585.1
temperature (K)	296(2)
λ (Å)	0.71073
crystal system	Monoclinic
space group	$P2_1/c$
a (Å)	9.6134(2)
b (Å)	20.2505(4)
c (Å)	11.6483(3)
β (deg)	97.520(1)
V (Å^3)	2248.14(9)
Z	4
D_{calcd} (Mg m^{-3})	1.729
μ (mm^{-1})	1.38
F(000)	1184
R_1 [$I > 2\sigma(I)$]^a	0.029
R_2 [$I > 2\sigma(I)$]^b	0.078
GOF on F^2	1.07

$^aR_1 = \Sigma||F_o| - |F_c||/\Sigma|F_o|$. $^bR_2 = \{\Sigma[w(F_o^2 - F_c^2)^2/\Sigma w(F_o^2)^2]\}^{1/2}$; $w = 1/[\sigma^2(F_o^2) + (0.0393P)^2 + 1.5954P]$, where $P = (F_o^2 + 2F_c^2)/3$.

Quantum Mechanical Calculations. The geometries for pseudo-octahedral [M(bppd)]$^+$ five trivalent metal ions have been optimized in the gas phase using ab initio Hartree−Fock (HF) HF/6-31G* and HF/SDD methods.[25] These calculation were also performed for the [Co(bped)]$^+$ complex ion. The HF/SDD method combines Stuttgart effective core potential for core electrons with Dunning's D95 basis set for valence electrons.[26−29] The electron correlation energy was evaluated at the MP2/6-31G*//HF/6-31G* and MP2/SDD//HF/SDD levels.[25] The solvation free energies were calculated using the polarized continuum model (PCM) and dielectric constant of water (ε = 78.5)[30] for the HF/6-31G* and HF/SDD wave functions. All quantum mechanical calculations were carried out using the Gaussian 03 program.[31]

RESULTS

Syntheses. *N,N′*-Bis(2-pyridylmethyl)-1,3-diaminopropane-*N,N′*-diacetic acid was previously prepared by Kanamori

dx.doi.org/10.1021/ic402810e | Inorg. Chem. 2014, 53, 3404−3416

Scheme 1. General Synthetic Procedure for Preparing H_2bppd

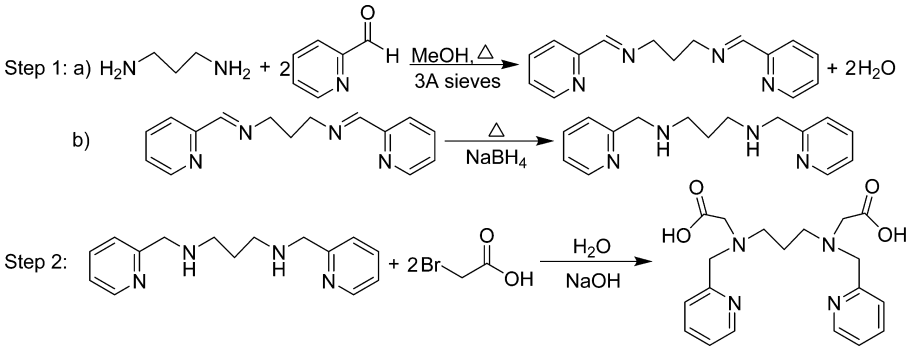

and co-workers using concentrated perchloric acid to isolate the compound as a $HClO_4$ solvate.[14] This synthetic procedure introduces the acetic acid functionalities to the pyridylmethyl-substituted diamine using chloroacetic acid. The product was obtained in relatively low yield (40%) and characterized by elemental analysis and infrared spectroscopy.

The reactions successfully carried out in the present study are summarized in Schemes 1 and 2.

Scheme 2. Synthetic Procedure for Preparing Metal−bppd^{2-} Compounds

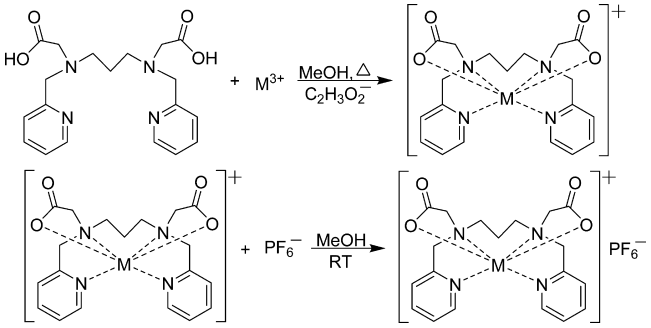

Scheme 1 shows the facile, two-step procedure for the synthesis of H_2bppd using simple starting reagents that employs bromoacetic acid, a strong alkylating agent, to provide improved yields. Step 1 of the synthesis is a sequential, one pot preparation of the 2-pyridylmethyl-substituted diamine, bpmdap, that builds upon earlier synthetic work reported by Nash and co-workers.[9] In the synthesis of the precursor diamine, activated molecular sieves are used to drive the reaction to completion by scavenging the water produced during formation of the diimine. Reduction of the diimine to the diamine is nearly quantitative and the di-2-methylpyridyl-substituted product, bpmdap, is obtained in high purity. Step 2 of the synthesis involves elaboration of the diamine to the diacetic acid using two equivalents of bromoacetic acid. Reaction of the diamine with bromoacetic acid leads cleanly to the desired diacetic acid product in good yield (60%). The use of bromoacetic acid results in higher yields than those obtained using chloroacetic acid as the alkylating agent.[14] This two-step synthetic procedure is readily extended to diamines with different backbones, for example, H_2bped (yield 77%). The ion exchange chromatography used to remove the sodium halide byproducts of the alkylation reaction results in the diamine product being isolated as a hydrochloride, which is hygroscopic.

H_2bppd was characterized by elemental analysis, equivalent weight titration, infrared spectroscopy, and ^{1}H and ^{13}C NMR spectroscopy. The infrared spectrum of H_2bppd shows a strong, very broad band in the 3400−2500 cm^{-1} region characteristic of strongly hydrogen bonded −OH and −NH$^+$ functionalities. Bands indicative of carboxylic acid and pyridyl groups are also present. The ^{1}H NMR spectrum of H_2bppd shows eight resonances with the expected relative intensities and splitting patterns at chemical shift values characteristic of a poly-aminocarboxylic acid with aromatic substituents. These signals appear at decreasing field strength as a pentuplet, a triplet, a singlet, a singlet, a triplet, a doublet, a triplet of doublets, and a doublet of triplets. Ten resonances are observed in the ^{13}C NMR spectrum in the expected regions. These resonances were assigned on the basis of COSY and HSQC experiments.

Scheme 2 shows the synthesis for Group 13 trivalent metal complexes with the fully deprotonated ligand. This synthesis, which is carried out in anhydrous methanol, starts by neutralizing the five acidic hydrogen atoms of the isolated H_2bppd·3HCl with sodium acetate. In this case, the reaction is carried out under reflux conditions to improve the kinetics of metal complexation. The complex ion, [M(bppd)]$^+$, precipitates out of solution upon addition of the PF_6^- counterion. The syntheses of the monoprotonated metal−ligand complex ions, [M(Hbppd)Cl]$^+$, are conducted in an analogous fashion employing the stoichiometric amount of sodium acetate that only neutralizes the HCl solvate.

The Ln[bppd]$^+$ salts were prepared in a similar manner with the reaction carried out at room temperature to prevent the inclusion of inorganic salts.[4] No crystalline samples of the lanthanide compounds suitable for X-ray crystallography analysis could be prepared despite trying a variety of different solvents (H_2O, MeOH, EtOH, PrOH, and CH_3CN), solvent mixtures (*n*-BuOH/H_2O, CH_3CN/H_2O), and crystal growth techniques (slow evaporation, slow cooling, vapor diffusion, and liquid−liquid interface diffusion). A Co(III)-bppd^{2-} compound, [Co(bppd)]PF_6, was also prepared as previously described for use as an aid to differentiate among different types of carboxylate bonding and cis and trans geometric isomers.[21] The [M(bppd)]PF_6 compounds were characterized by elemental analysis, mass spectrometry, infrared spectroscopy, and ^{1}H and ^{13}C NMR spectroscopy. All of these complexes gave acceptable elemental analysis except for the [Al(bppd)]-PF_6, which is hygroscopic. The [M(Hbppd)Cl]PF_6 compounds were characterized by mass spectrometry and infrared spectroscopy.

Mass Spectra. The mass spectra of the Group 13 metal compounds [M(bppd)]PF_6 give strong peaks identified as the

dx.doi.org/10.1021/ic402810e | Inorg. Chem. 2014, 53, 3404−3416

parent molecular ion at m/e values with the isotope distribution and relative intensity patterns expected for metal complexes of the stated stoichiometry. For these compounds, this is the most intense signal in the mass spectrum. For the lanthanide compounds $[Ln(bppd)]PF_6$ and $[Al(Hbppd)Cl]PF_6$ the intensity of the signal at the m/e value for the parent molecular ion is very weak. The most intense signal in the spectra of these compounds is at the m/e value of 373.3 (H_2bppd + 1), which suggests weaker metal−bppd^{2-} bonding. The mass spectra of the gallium and indium compounds containing a monoprotonated acetate group, $[M(Hbppd)Cl]PF_6$ for M = Ga, In, show peaks at m/e values for the parent molecular ion with the expected isotope distribution patterns as well as peaks at m/e values identified as the fully deprotonated complex ion $[M(bppd)]^+$. No signals were observed in the mass spectra of these compounds at m/e values corresponding to uncoordinated ligand.

Infrared Spectra. The infrared spectra of the isolated metal-bppd^{2-} compounds are all very similar without obvious features that might be used to discriminate between cis and trans isomers. All compounds exhibit absorption bands in regions characteristic of aromatic and aliphatic stretching, bending, and deformation modes, carboxylate stretching modes, and frequencies associated with the PF_6^- anion, that is, ∼915, 840, and 555 cm^{-1}.[32] The IR spectra of the *cis*-O,O; *cis*-N_{py},N_{py} $[Ga(bppd)]^+$ complex and the *trans*-O,O $[Co(bppd)]^+$ complex are nearly identical. The spectrum of the *cis*-O,O; *cis*-N_{py},N_{py} $[Ga(bppd)]^+$ ion shows a shoulder at ∼1363 cm^{-1} that is not apparent in the *trans*-O,O $[Co(bppd)]^+$ complex, Supporting Information Figure S2. In both cases, however, the antisymmetric COO^- stretching mode appears as a very strong, broad, featureless band in the 1685−1660 cm^{-1} region. Thus, the band splitting that might be expected for a lower symmetry cis complex is not observed. The infrared spectra of the monoprotonated $Hbppd^-$ complexes of Al(III), Ga(III), and In(III), $[M(Hbppd)]^{2+}$, show an additional strong band in the −O−H stretching region (∼3500 cm^{-1}) and another in the C═O stretching region (∼1730 cm^{-1}). Complexes isolated as hydrates also exhibit absorption bands in regions characteristic of water of hydration that is best observed in the mull spectra.

Frequencies and tentative assignments of the absorption bands in the 3500−1300 cm^{-1} region of the IR spectra are given in the Experimental Section with the characterization data for each compound isolated. In metal complexes of simple amino acids, the carboxylate stretching bands can often be assigned empirically without difficulty. Carboxylate stretching modes also give rise to the bands most sensitive to the effect of metal ion complexation. This is especially true for the antisymmetric COO^- stretching mode, ν_a. The symmetric COO^- stretching mode, ν_s, is less sensitive to complexation and its assignment can be problematic. To alleviate the uncertainty associated with identifying the symmetric COO^- stretching mode, bands assignable to this mode were identified empirically by comparison of the spectrum of $[Co(bppd)]^+$ and all other metal−bppd^{2-} complexes with the spectrum of the Co(III) complex ion of the precursor diamine bpmdap, $[Co(bpmdap)Cl_2]^+$. No bands in 1400−1300 cm^{-1} region, where a symmetric COO^- stretching mode is expected to occur, appear in the infrared spectrum of $[Co(bpmdap)Cl_2]^+$. This allows explicit identification and assignment of the symmetric COO^- stretching band in the $[M(bppd)]^+$ and $[M(Hbppd)Cl]^+$ complexes. Carboxylate stretching frequencies along with the difference between the antisymmetric and symmetric stretching bands, $\Delta\nu = \nu_a(COO^-) - \nu_s(COO^-)$, for the isolated metal compounds are given in Table 2.

Table 2. Carboxylate Stretching Frequencies, ν, and $\Delta\nu$ Values for Selected $[M(bppd)]^+$ and $[M(Hbppd)Cl]^+$ Complexes

metal ion	ν(C═O)	$\nu_a(COO^-)$	$\nu_s(COO^-)$	$\Delta\nu$ (cm^{-1})
Na_2bppd		1588	1405	183
$[Al(bppd)]^+$		1670	1385	285
$[Ga(bppd)]^+$		1683	1348	335
$[In(bppd)]^+$		1644	1384	260
$[Al(Hbppd)Cl]^+$	1735	1636	1395	241
$[Ga(Hbppd)Cl]^+$	1734	1653	1384	269
$[In(Hbppd)Cl]^+$	1731	1608	1384	224
$[La(bppd)]^+$		1601	1413	188
$[Nd(bppd)]^+$		1603	1414	189
$[Sm(bppd)]^+$		1603	1414	189
$[Dy(bppd)]^+$		1605	1414	191

X-ray Structure. X-ray quality crystals of $[Ga(bppd)]PF_6$ were grown by slow evaporation of a supersaturated methanol solution in air at 16 °C. The compound crystallized in the monoclinic space group $P2_1/c$ with one molecule in the asymmetric unit and four asymmetric units per unit cell. The cation and anion are well resolved in the structure, although some disorder is noted in the anion. Relevant crystallographic information is shown in Table 1 and in the Supporting Information. A displacement ellipsoid plot of the $[Ga(bppd)]^+$ cation is shown in Figure 2. The Ga atom is surrounded by the ligand in an approximately octahedral environment of general formula GaN_4O_2. The coordination environment can be described as *cis*-O,O; *cis*-N_{py},N_{py} with the acetate groups coordinated in a monodentate fashion. Selected bond distances and angles are shown in Table 3.

Table 3. Selected Bond Distances (Å) and Angles (deg) for $[Ga(bppd)]PF_6$

Ga1−O1	1.9459 (15)	O1−Ga1−O3	91.83 (7)
Ga1−O3	1.8956 (14)	O1−Ga1−N1	99.41 (7)
Ga1−N1	2.0156 (17)	O1−Ga1−N2	83.59 (7)
Ga1−N2	2.0673 (16)	O1−Ga1−N4	89.28 (7)
Ga1−N3	2.1377 (17)	N1−Ga1−N3	90.80 (6)
Ga1−N4	2.1061 (17)	N1−Ga1−N4	170.74 (6)
C8−O1	1.286 (3)	N2−Ga1−N4	96.47 (7)
C8═O2	1.211 (3)	O2═C8−O1	125.0 (3)
C19−O3	1.287 (3)	O4═C19−O3	123.5 (2)
C19═O4	1.208 (3)	C8−O1−Ga1	117.81 (15)
		C19−O3−Ga1	114.77 (14)

Quantum Mechanical Calculations. To examine structure−property relationships involved in metal−ligand selectivity, the gas-phase and aqueous solution energetics were calculated for the three geometric isomers possible for a pseudo-octahedral $[M(bppd)]^+$ complex ion with six different trivalent cations. The results of the calculations relative to the *trans*-O,O isomer are given in Table 4 along with the results for the $[Co(bped)]^+$ cation.

The solvation free energies (kcal/mol), ΔG_{solv}, that are presented in Table 4 are defined as the standard free energy of transfer of 1.0 M solute from the gas-phase to water.[33] These

dx.doi.org/10.1021/ic402810e | Inorg. Chem. 2014, 53, 3404−3416

Table 4. Calculated Energies (kcal/mol), Charges (au), Distances (Å), and Angles (deg) for $[M(bpad)]^+$ Cations

	property	$[Co(bped)]^+$ HF/6-31G*	$[Co(bppd)]^+$ HF/6-31G*	$[Al(bppd)]^+$ HF/6-31G*	$[Ga(bppd)]^+$ HF/6-31G*	$[Ga(bppd)]^+$ HF/SDD	$[In(bppd)]^+$ HF/SDD	$[La(bppd)]^+$ HF/SDD
trans-O,O	ΔG_{solv}	−52.7	−51.3	−49.2	−49.9	−57.8	−59.4	−79.4
	charge of M[a]	1.66	1.69	1.63	1.80	1.74	1.62	2.28
	M−O	1.853	1.850	1.807	1.865	1.884	2.013	2.240
	$M-N_{py}$	2.012	2.012	2.068	2.076	2.088	2.194	2.672
	M−N	1.978	2.005	2.097	2.129	2.170	2.283	2.729
	N−M−N angle[b]	108.6	100.4	104.1	103.9	105.6	111.3	146.5
cis-O,O; *cis*-N_{py},N_{py}	ΔG_{solv}	−59.4	−55.9	−52.9	−54.8	−61.8	−63.0	−82.6
	$\Delta\Delta G_{solv}$[c]	−6.7	−4.6	−3.7	−4.9	−4.0	−3.6	−3.2
	ΔE_{SCF}[c]	12.7	6.3	5.1	6.8	6.0	6.4	6.1
	ΔE_{corr}[c]	−1.8	−0.5	−1.6	−2.3	−2.9	−3.1	−1.0
	ΔG in solution[c]	4.2	1.2	−0.2	−0.4	−0.9	−0.3	1.9
	charge of M[a]	1.67	1.70	1.67	1.77	1.75	1.63	2.26
	$M-O_3$[d]	1.836	1.834	1.788	1.870	1.860	1.987	2.242
	$M-O_1$[d]	1.847	1.844	1.811	1.879	1.895	2.013	2.237
	$M-N_3$[d]	2.049	2.047	2.171	2.096	2.188	2.284	2.682
	$M-N_1$[d]	1.979	1.972	2.015	2.025	2.027	2.166	2.702
	$M-N_2$[d]	1.973	2.032	2.121	2.148	2.193	2.307	2.762
	$M-N_4$[d]	2.007	2.011	2.096	2.118	2.155	2.272	2.738
	N−M−O angle[b]	103.9	94.5	98.3	97.9	100.0	108.4	143.4
trans-N_{py},N_{py}	ΔG_{solv}	−57.6	−56.9	−53.0	−54.2	−60.3	−60.5	−76.1
	$\Delta\Delta G_{solv}$[c]	−4.9	−5.6	−3.8	−4.3	−2.5	−1.1	3.3
	ΔE_{SCF}[c]	16.1	12.5	7.4	10.7	7.7	3.8	7.9
	ΔE_{corr}[c]	−0.3	0.3	−1.1	−3.6	−1.7	−1.2	−0.2
	ΔG in solution[c]	10.9	7.2	2.5	2.8	3.5	1.3	11.0
	charge of M[a]	1.70	1.73	1.67	1.77	1.78	1.64	2.25
	M−O	1.862	1.850	1.759	1.876	1.870	1.997	2.265
	$M-N_{py}$	2.002	2.002	2.074	2.075	2.091	2.203	2.648
	M−N	2.020	2.051	2.182	2.172	2.273	2.359	2.764
	O−M−O angle[b]	106.9	97.1	106.8	105.2	112.5	120.7	149.6

[a]Mulliken charge calculated for the complex in the gas-phase. [b]X−M−Y describes the open angle formed by donor atoms trans to the N atoms of the diamine, where X = N_{py} or O and Y = N_{py} or O. [c]Relative to the *trans*-O,O isomer (eq 1). [d]For labeling, see Figure 2.

free energies can be effectively combined with ab initio gas-phase energetics to predict equilibrium or rate constants for chemical reactions in aqueous solution.[34] The difference between the solvation free energy for a *trans*-N_{py},N_{py} (or *cis*-O,O; *cis*-N_{py},N_{py}) isomer and ΔG_{solv} values of the *trans*-O,O isomer gives $\Delta\Delta G_{solv}$, that is, the solvation free energy of that isomer relative to the *trans*-O,O isomer. $\Delta\Delta G_{solv}$ is used to calculate ΔG in solution for the indicated isomer relative to the *trans*-O,O isomer, eq 1.

$$\Delta G \text{ in solution} = \Delta\Delta G_{solv} + \Delta E_{SCF} + \Delta E_{corr} \quad (1)$$

where $\Delta\Delta G_{solv}$ is the relative solvation free energy calculated at the PCM level, ΔE_{SCF} is the relative self-consistent field energy calculated at the HF level, and ΔE_{corr} is the relative electron correlation energy calculated at the MP2 level.

The calculated metal charges (au), metal−ligand bond distances (Å), and the open bond angle (deg) formed by the O or N_{py} donor atoms trans to the N atoms of the diamine, the X−M−Y angle, for the $[M(bppd)]^+$ and $[Co(bped)]^+$ complex ions are also given in Table 4. These physical parameters are useful for testing the validity of assumed coordination numbers as well as providing insight into the nature of metal−ligand bonding. For these considerations, it is important to note that the HF method tends to systematically overestimate M−O distances by about 0.03 Å compared to the more accurate MP2 method.[35]

NMR Spectroscopy. The ^1H and ^{13}C assignments for H_2bppd and the trivalent metal−$bppd^{2-}$ complexes were made on the basis of 2D COSY, NOESY, and HSQC experiments. The COSY and HSQC experiments established the detected $^1H-^1H$ and $^1H-^{13}C$ correlations (Supporting Information Figures S3−S6), whereas the 2D NOESY experiments established the spatial proximity of the hydrogen atoms within the complexes (Supporting Information Figures S7 and S8). The ^1H and ^{13}C NMR data obtained for H_2bppd and the Co(III), Al(III), In(III), La(III), and Ga(III) complexes in D_2O at 25.0 °C are presented in Table 5 and Supporting Information Table S1. H_2bppd shows 8 resonances in the ^1H NMR spectrum and 10 of the possible 19 resonances in the ^{13}C NMR spectrum. The Al(III) and La(III) complexes show 8 resonances in the ^1H spectrum, while the Co(III) and In(III) complexes show 11 and 10 ^1H resonances, respectively. Each of these complex ions also displays 10 of the possible 19

dx.doi.org/10.1021/ic402810e | Inorg. Chem. 2014, 53, 3404−3416

Table 5. ^{1}H NMR (500 MHz) Spectral Data (ppm)[a,b] for H_2bppd and Its Co(III), Al(III), In(III), La(III), and Ga(III) Complexes in D_2O at 25 °C

	H_2bppd·3HCl	[Co(bppd)]$^+$	[Al(bppd)]$^+$	[In(bppd)]$^+$	[La(bppd)]$^+$	[Ga(bppd)]$^+$
H(1)	8.75 (5.7, 0.8)	8.79 (5.5)	8.61 (4.5)	8.94 (5.5)	8.63	8.89 (5.5)
H(2)	7.92 (6.8)	7.87 (6.5)	7.56 (6.5)	7.75 (6.5)	7.57	8.04 (6.3)
H(3)	8.44 (7.8, 2.5)	8.32 (7.8, 1.3)	8.00 (7.8, 1.8)	8.20 (8.0, 1.5)	8.02	8.50 (8.0, 1.5)
H(4)	7.97 (8.1)	7.94 (8.0)	7.61 (8.0)	7.70 (8.0)	7.62 (7.5)	7.98 (8.0)
H(6a)	4.53	4.94 (16)	4.54	4.41 (16)	4.52	4.65 (19)
H(6b)		4.62 (16)		4.14 (16)		4.29 (19)
H(7a)	3.88	3.58 (20)	3.77	3.69 (18)	3.76	4.21 (17)
H(7b)		3.54 (20)		3.35 (18)		3.68 (17)
H(9a)	3.14 (7.5)[c]	3.16 (15)	3.32 (7.5)[c]	3.16 (5.3)[c]	3.29	3.50 (8.5)
H(9b)		3.08 (15)				2.80 (8.5)
H(10)	2.00 (7.6)	2.77 (4.9)	2.21 (7.0)	2.16 (5.0)	2.20	2.38 (6.5)
H(11a)						3.79 (9.0)
H(11b)						3.25 (8.0)
H(12)						7.34 (5.5)
H(13)						7.55 (6.5)
H(14)						8.27 (7.8, 1.5)
H(15)						7.82 (8.5)
H(17a)						5.13 (19)
H(17b)						4.70 (19)
H(18a)						4.04 (17)
H(18b)						3.93 (17)

[a]For labeling, see Figure 2. Resonances of the *ProR* and *ProS* diastereotopic protons are differentiated in the labeling as a and b, respectively. [b]Numbers in parentheses refer to ($^3J_{HH}$, $^4J_{HH}$) coupling for H(1−4, 10, 12−15) and ($^2J_{HH}$) coupling for H(6−9, 11, 17−18) in Hz. [c]Coupling for H(9a) is reported as ($^3J_{HH}$) coupling.

resonances in its ^{13}C NMR spectrum. The Ga(III) complex, which adopts a *cis*-O,O; *cis*-N_{py},N_{py} geometry with only the identity symmetry element present, shows 21 ^{1}H and 19 ^{13}C resonances. In the case of the Co(III), In(III), and Ga(III) complexes, the individual hydrogen atoms at the methylene positions, H(6), H(7), and H(9), are nonequivalent diastereotopic protons that experience geminal coupling ($^2J_{HH}$), see Figure 2 for labeling. All resonances observed in each complex ion show the expected splitting patterns, intensities, and chemical shifts characteristic of a polyaminocarboxylate ligand bearing the 2-methylpyridyl functionality. The ^{1}H and ^{13}C spectra for [Sm(bppd)]$^+$ and [Nd(bppd)]$^+$ are very similar to that of [La(bppd)]$^+$, suggesting similar structures, but with increased line broadening due to the paramagnetic nature of these metal ions. The NMR spectral data for these [Ln(bppd)]$^+$ complex ions are given in the Experimental Section. NMR spectra were not attainable for [Dy(bppd)]$^+$ because the $^6H_{15/2}$ ground state for Dy(III) makes this complex ion very strongly paramagnetic.

DISCUSSION

X-ray Structure. Crystals grown under three different sets of conditions with subtly different habits (needles vs blocks) were all examined via X-ray diffraction and afforded the same unit cell reported here (data not shown). The Ga atom is surrounded by the ligand in a distorted octahedral geometry provided by a N_4O_2 donor set. Selected bond distances and angles are shown in Table 3. The Ga−O distances of 1.8956 (14) and 1.9459 (15) Å are slightly shorter than the 1.945 Å average for the 56 reported GaN_4O_2 structures in the Cambridge Structural Database.[36] They are, however, well within the 1.823−2.475 Å range typical for the other 1205 structures with reported Ga−O distances, which is the same range as the 822 reported Ga−O carboxylate distances. The Ga−N distances are 2.0673 (16) and 2.1061 (17) Å for the diamine and 2.0156 (17) and 2.1377 (17) Å for the pyridyl units. These values are typical for GaN_4O_2 structures (1.852−2.194 Å) and for the vast majority of the 1594 structures with reported Ga−N distances (1.701−2.434 Å) in the Cambridge Structural Database.[36] All but one of the bonds in the database for the 662 reported Ga−N_{pyr} distances fall in the range 1.819−2.434 Å and all but one of the 3708 Ga−NR_2 bond lengths lie in the range 1.816−2.686 Å. Many of the angles of the N_4O_2 coordination sphere around Ga deviate significantly from ideal octahedral values. For example in Table 3, although the O1−Ga1−O3 and the pyridyl N1−Ga1−N3 angles are close to ideal, the deviation for the diamine N2−Ga1−N4 angle is much larger and the O1−Ga1−N2 angle is much smaller than ideal.

Although we previously reported a structure for [Co(bppd)]-PF_6,[21] there is little other structural data available for bppd^{2-} complexes to which the [Ga(bppd)]PF_6 structure can be compared. In the cobalt complex, the Co has a distorted octahedral coordination geometry provided by a N_4O_2 donor atom set with the bppd^{2-} ligand chelating in a *trans*-O,O configuration, Figure 1. In the present case, the N_4O_2 donor atom set of bppd^{2-} chelates Ga in a *cis*-O,O; *cis*-N_{py},N_{py} fashion with a somewhat more distorted octahedral coordination geometry than in the Co(bppd)$^+$ cation.

Quantum Mechanical Calculations. The results of the quantum mechanical calculations indicate that in gas-phase the *trans*-O,O isomer (C_2 symmetry) is the most stable of the three possible isomers. In aqueous solution, the stability of the *trans*-O,O isomer becomes fairly similar to the *cis*-O,O; *cis*-N_{py},N_{py} isomer (C_1 symmetry), while remaining more stable than the *trans*-N_{py},N_{py} isomer (C_2 symmetry) for all of the metal complexes listed in Table 4. The ΔG in solution values, eq 1, for the [Co(bped)]$^+$, [Co(bppd)]$^+$, and [Ga(bppd)]$^+$ complexes correctly predict the lowest energy isomer as the isomer

dx.doi.org/10.1021/ic402810e | Inorg. Chem. 2014, 53, 3404−3416

observed by X-ray crystallography, that is, the *trans*-O,O, *trans*-O,O, and *cis*-O,O; *cis*-N_{py},N_{py} isomers, respectively. The M−O and M−N bond distances and X−M−Y angles calculated for these geometries are very similar to observed values.[3,16,17,22] These results indicate that the systematic errors in the calculated free energies for complexes with different metal ions and different geometries are similar. Specifically, the errors involve the use of gas-phase geometries, energetics at 0 K, and a simplified description of the solvent, as well as wave function and electron correlation.

Unfortunately, the experimental validation of the PCM/MP2/6-31G*//HF/6-31G* methodology is not directly applicable to the calculations for the In(III) and La(III) complexes that were performed using a smaller SDD basis set. The SDD basis set lacks polarization functions and approximates core electrons simply by using an effective core potential. This methodological change was necessary because the 6-31G* basis set is available only for elements in the first four periods of the periodic table. The calculations were performed for the $[Ga(bppd)]^+$ complex using both HF/6-31G* and HF/SDD basis sets to establish a seamless transition from one basis set to the other. Although the MP2 energy is usually the physical parameter most sensitive to basis set deficiencies, the MP2/6-31G* and MP2/SDD methods yield similar ΔE_{corr} values, −2.3 and −2.9 kcal/mol, respectively, for the relative correlation energy of the *cis*-O,O; *cis*-N_{py},N_{py} $[Ga(bppd)]^+$ isomer. Since the effect of the basis set on the sum of $\Delta\Delta G_{solv}$ and ΔE_{SCF} is negligible in this case, methods utilizing either basis set correctly predict the observed all cis geometry for $[Ga(bppd)]^+$. The ΔG in solution value obtained by the PCM/MP2/6-31G*//HF/6-31G* method, however, is somewhat less favorable (−0.4 kcal/mol) than that obtained by the PCM/MP2/SDD//HF/SDD method (−0.9 kcal/mol). This dual calculation approach provides a means of correcting for systematic errors introduced in ΔG values for $[In(bppd)]^+$ and $[La(bppd)]^+$ when using the HF/SDD method, which is necessitated by the large number of core electrons. The correction for $[In(bppd)]^+$ and $[La(bppd)]^+$ makes ΔG 0.5 kcal/mol more positive than those obtained directly from the HF/SDD calculations. While this has no effect on the prediction of a *trans*-O,O geometry for $[La(bppd)]^+$, the correction makes the calculated ΔG in solution value for the all cis$[In(bppd)]^+$ isomer less favorable than the *trans*-O,O isomer by 0.2 kcal/mol. Parenthetically, the ^1H and ^{13}C NMR spectra of the isolated $[In(bppd)]PF_6$ compound indicate that the cation in solution has C_2 symmetry, which is consistent with this correction.

Calculations for a six-coordinate $[La(bppd)]^+$ complex converge to a *trans*-O,O structure with a very large N_{py}−La−N_{py} bond angle (146.4°), a high metal charge (2.28 au), and a high solvation free energy (−79.4 kcal/mol). It is evident that the pendant arms of the attached acetate and pyridylmethyl groups are not long enough to encapsulate the larger La(III) ion at the center of a pseudo-octahedral arrangement of donor atoms. The geometric arrangement of the $bppd^{2-}$ ligand around La in this configuration is best described as a nestlike structure with a large open space in La's coordination sphere available for additional ligands, for example, two H_2O molecules, Figure 3. This allows the La to achieve a more preferred coordination number. This structure is consistent with the stoichiometry of the isolated La salt, $[La(bppd)]PF_6{\cdot}2H_2O$, the IR and mass spectrometry data, and the ^1H and ^{13}C NMR spectra, which indicate a La−$bppd^{2-}$ species in solution of C_2 symmetry.

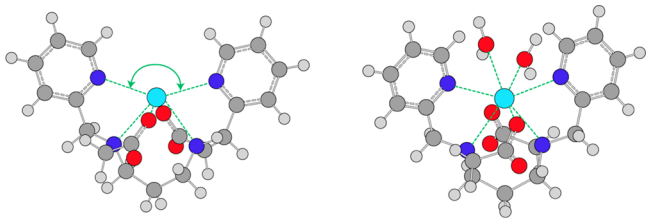

Figure 3. Two structures of the $[La(bppd)]^+$ complex that were fully optimized by HF/SDD calculation in the absence and explicit presence of two H_2O molecules. The open X−M−Y angle for the *trans*-O,O $[La(bppd)]^+$ complex (left) and the nestlike structure that allows the larger La(III) ion to achieve the more preferred coordination number of 8 in $[La(bppd)(H_2O)_2]^+$ (right).

The QM results for $[Al(bppd)]^+$ show the calculated solvation free energies, ΔG_{solv}, for the three geometric isomers possible for a pseudo-octahedral Al(III) complex ion to be the least energetically favorable of the six trivalent cations investigated. The *cis*-O,O; *cis*-N_{py},N_{py} isomer is predicted to be more stable (−0.2 kcal/mol) than the *trans*-O,O isomer, whereas the ^1H and ^{13}C NMR spectra suggest a single, higher symmetry species in solution. The calculated Al−O distances for all three isomers are in the expected range (1.516−2.736 Å) and close to the expected mean value (1.824 Å).[36] The Al−N distances are in the expected range (1.657−2.891 Å), but ∼0.1 Å larger than the expected mean (1.957 Å).[36] The average of the calculated Al−N distances for the *trans*-O,O, and *trans*-N,N isomers are 2.083, 2.101, and 2.128 Å, respectively. All of the $[Al(bppd)]^+$ isomers have relatively large steric repulsions between the aromatic rings of the coordinated 2-pyridylmethyl groups because of Al(III)'s small size. These steric repulsion are evident in the crystal structures of $[Co(bped)]^+$,[3] $[Co(bppd)]^+$,[21] and $[Ga(bppd)]^+$ through the pitch and position of the pyridine rings. In fact, repulsions between the pyridine rings are present in the *trans*-O,O and *cis*-O,O; *cis*-N_{py},N_{py}, isomers for all 6 complexes investigated; however, they are greatest for the $[Al(bppd)]^+$ isomers. The ring repulsions in the gas-phase geometry of the *trans*-O,O $[Al(bppd)]^+$ isomer are ∼1 kcal/mol greater than for the *cis*-O,O; *cis*-N_{py},N_{py}, isomer and this energy difference is carried forward into ΔG in solution. Thus, a factor that must be considered when using the energies calculated for different $[Al(bppd)]^+$ geometries is the relatively larger steric repulsion in complexes with the smaller, oxophilic Al(III) ion. The 2-pyridylmethyl groups are the substituents most likely to be displaced in aqueous solution as the affinity of Al for neutral nitrogen donor groups is known to be low.[37] Indeed, the QM calculations indicate that exchange of two pyridine donor groups for two water molecules, Figure 4 (right), is favored in aqueous solution by 0.7 kcal/mol. This

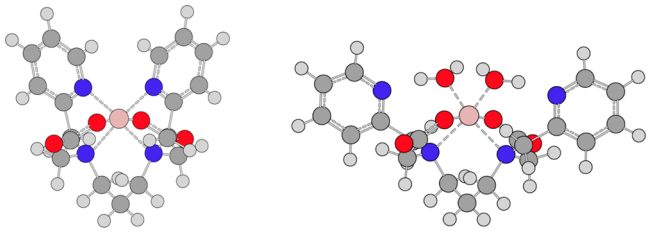

Figure 4. A comparison of the structures for six-coordinated *trans*-O,O $[Al(bppd)]^+$ complexes with direct pyridine-Al(III) bonding (left) and with both pyridine groups replaced by H_2O (right).

dx.doi.org/10.1021/ic402810e | *Inorg. Chem.* 2014, 53, 3404−3416

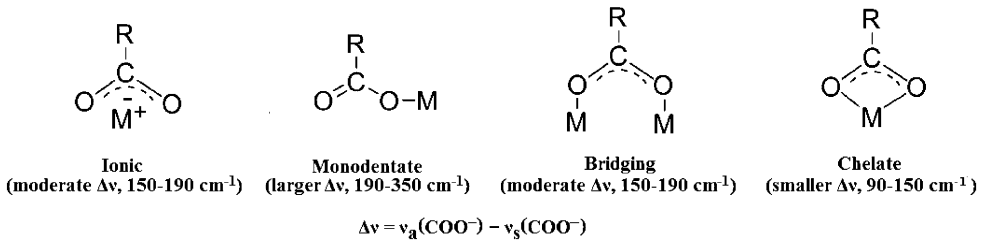

Figure 5. Idealized metal−ligand bonding modes and characteristic frequency range between the COO^- stretching bands, $\Delta\nu$, for an acetate functionality.[41]

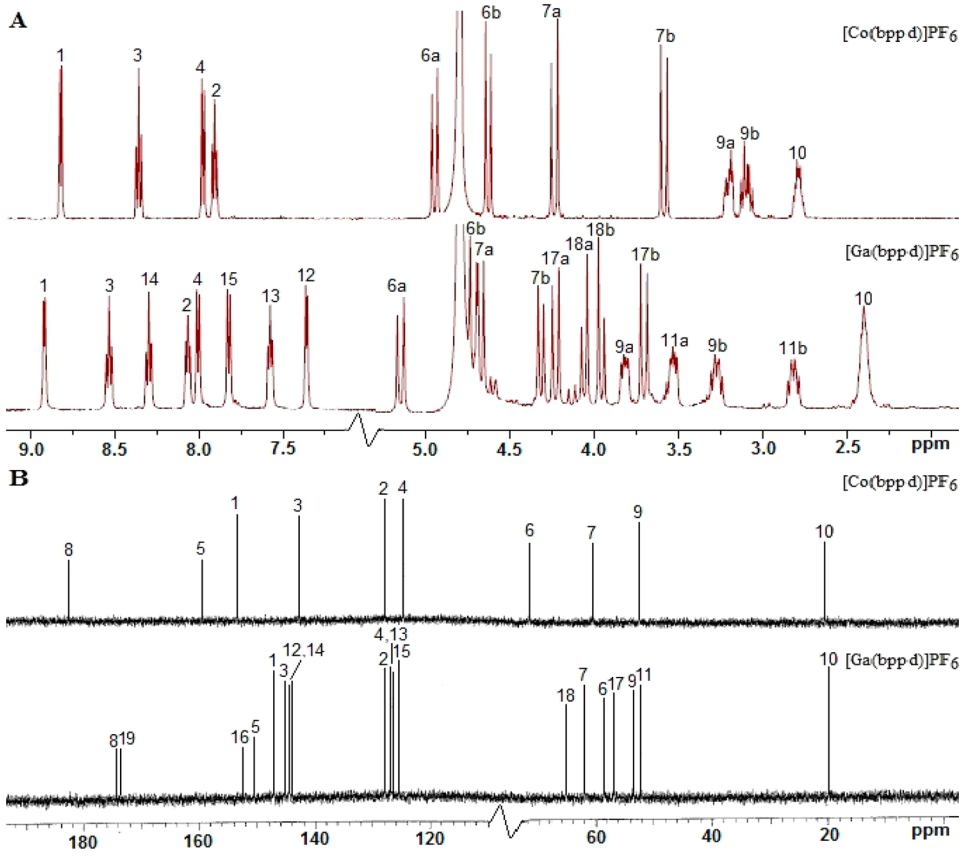

Figure 6. ^1H and ^{13}C spectra, A and B, respectively, of *trans*-O,O [Co(bppd)]PF_6 stacked above *cis*-O,O; *cis*-N_{py},N_{py} [Ga(bppd)]PF_6 in D_2O at 25 °C. See Figure 2 for labeling.

favorable free energy is driven by a favorable relative gas-phase energy (ΔE_{SCF} = −3.9 kcal/mol), a favorable relative electron correlation energy (ΔE_{corr} = −9.4 kcal/mol) because of the replacement of the Al−N bonds by Al−O bonds, and favorable intramolecular pyridine−water hydrogen-bonding interactions that is opposed by the desolvation of two water molecules ($\Delta\Delta G_{solv}$ = 12.6 kcal/mol). Thus, a plausible explanation of the NMR results is that in solution the coordinated 2-pyridylmethyl groups are replaced by two water molecules, Figure 4. This ligand exchange leads to a lower overall energy and a *trans*-O,O isomer with C_2 symmetry.

Infrared Spectra. The mid-infrared spectra of $[M(bppd)]^+$ complexes are too similar to be used to distinguish between *trans*-O,O (C_2 symmetry) and *cis*-O,O; *cis*-N_{py},N_{py} (C_1 symmetry) isomers. For soluble metal-$bppd^{2-}$ compounds, the best spectroscopic method to discriminate between cis and trans isomers appears to be ^1H and ^{13}C NMR spectroscopy (vide infra).[3] For insoluble salts, it might be possible to develop a vibrational criterion based on symmetry arguments regarding the number of metal−nitrogen and metal−oxygen stretching absorptions appearing in the far-infrared region to make this distinction as reported for copper−amino acid complexes.[38]

Three idealized, symmetric types of carboxylate binding for a coordinated acetate group, monodentate, bidentate, and bridging, are shown in Figure 5 along with stylized ionic bonding. Monodentate coordination removes the equivalence of the two O atoms in an acetate ion. This should increase the antisymmetric stretching frequency, decrease the symmetric stretching frequency, and increase the separation between these two bands, $\Delta\nu = \nu_a(COO^-) - \nu_s(COO^-)$, relative to an ionic acetate. Symmetrical bridging or chelation should shift both stretching frequencies in the same direction and decrease the separation between the bands.[39] This type of analysis can be used to rationalize the empirical correlation between the magnitude of $\Delta\nu$ and different types of COO^- binding modes.[40] The assignment of the antisymmetric and symmetric

dx.doi.org/10.1021/ic402810e | Inorg. Chem. 2014, 53, 3404−3416

Table 6. Spatial Proximity of Definitive Hydrogen Atoms for the *trans*-O,O and *trans*-N_{py},N_{py} Isomers of $[Co(bppd)]^+$ and $[In(bppd)]^+$[a]

$[M(bppd)]^+$ complex	H(7) – H(10)	H(6) – H(10)	H(1) – H(18)
trans-O,O $[Co(bppd)]^+$	2.39	4.38	5.93
trans-O,O $[In(bppd)]^+$	2.51	4.38	6.35
trans-N_{py},N_{py} $[Co(bppd)]^+$	4.45	2.14	2.88
trans-N_{py},N_{py} $[In(bppd)]^+$	4.42	2.20	3.62

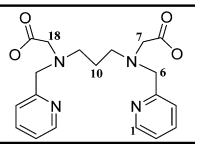

[a]Nonbonding H−H distances (Å) were determined from the atomic coordinates obtained from the HF/6-31G* calculations.

stretching bands in spectra of $[M(bppd)]^+$ and $[M(Hbppd)Cl]^+$ complexes was achieved by comparison with the spectrum of the $[Co(bpmdap)Cl_2]^+$ complex in the carboxylate stretching region.

Monodentate coordination of a single acetate oxygen atom is expected to result in an increase in the magnitude of $\Delta\nu$ compared to that for ionic salts and other types of acetate complexation. The IR results in Table 2 for Al(III), Ga(III), and In(III) $[M(bppd)]^+$ complexes show significant increases in the antisymmetric stretching frequency and large $\Delta\nu$ values (335−224 cm^{-1}) that demonstrate this behavior. The $[M(Hbppd)Cl]PF_6$ compounds of Al(III), Ga(III), and In(III) also show this behavior. Monoprotonated complexes were first detected in solution as the $[Ga(Hbped)]^{2+}$ cation, which exists in two or three isomeric forms with a noncoordinated carboxylic acid functionality.[3] In the present case, monodentate coordination is clearly indicated for the deprotonated acetate group. The appearance of a C═O stretching band at ∼1730 cm^{-1} in the spectra of the isolated solids suggests the presence of an uncoordinated carboxylic acid functionality with the higher complex charge compensated by an additional anion.

The situation for the lanthanide compounds, which were all isolated as hydrates, is somewhat more complicated since their $\Delta\nu$ values lie within experimental error of the ranges expected for three idealized bonding modes. Further, several complexes with monodentate acetate groups without large $\Delta\nu$ values, that is, < 200 cm^{-1}, have been reported.[40,41] In each of these cases, the carboxylate oxygen not bonded to the metal ion is hydrogen-bonded to another ligand like H_2O that gives rise to a "pseudo-bridging" arrangement. For the $[Ln(bppd)]^+$ compounds reported in Table 2 both stretching bands shift in the same direction as expected for symmetrical bridging or chelation, but the separation between the two bands increases rather than decreases as expected. The $\Delta\nu$ values for the lanthanide compounds, which are nearly constant at ∼189 cm^{-1}, are only slightly higher than the $\Delta\nu$ value for the sodium−$bppd^{2-}$ salt (183 cm^{-1}). This strongly suggests that the lanthanide-COO^- bonding in these compounds is predominately ionic. This assessment is supported by the quantum mechanical calculations and the mass spectrometry results for the Ln(III)−$bppd^{2-}$ compounds, as well as the strong ionic nature of the bonding of f-element cations in aqueous solution with their ligands, including aminopolycarboxylates.[1]

NMR Spectroscopy. ^1H and ^{13}C NMR spectroscopy were used to characterize metal-$bppd^{2-}$ complexes and discriminate between cis and trans geometric isomers. A single species displaying C_2 symmetry was observed for all metal complexes investigated except for $[Ga(bppd)]^+$, which displays ^1H and ^{13}C resonances characteristic of the asymmetric *cis*-O,O; *cis*-N_{py},N_{py} isomer. The spectra reveal that the $[Ga(bppd)]PF_6$ product from the bulk synthesis, as well as the single crystals used for X-ray crystallographic analysis contain a single species of C_1 symmetry. The all cis isomer is easily distinguished from the trans isomers because of an approximate doubling in the number of resonances, Figure 6, observed because of its lack of symmetry. Distinguishing between *trans*-O,O and *trans*-N_{py},N_{py} isomers, which both have C_2 symmetry, is not possible using classical ^1H and ^{13}C NMR spectroscopy, however, it is possible to distinguish between the two trans isomers using 2D NOESY experiments.[3]

The chirality of the $bppd^{2-}$ ligand environment changes upon coordination to a metal ion, as observed in inorganic compounds with coordination geometries that feature the formation of chelate rings.[43,44] In the present case, $bppd^{2-}$ forms five chelate rings upon coordination to a metal center in a distorted octahedral geometry. This arrangement gives three sets of chelate rings that are both nonadjacent and noncoplanar around the metal center, which introduces chirality and makes the methylene protons H(6), H(7), and H(9) nonequivalent. This nonequivalency creates diastereotopic nuclei and allows for the possibility of resonances arising from both *Pro-R* and *Pro-S* hydrogen atoms.[45] Indeed, the presence of diastereotopic nuclei is evident in the ^1H NMR spectra of the $[M(bppd)]^+$ complexes, as well as the X-ray structure of $[Co(bppd)]PF_6$.[21]

Coordination of $bppd^{2-}$ to Co(III), In(III), and Ga(III) gives rise to distinguishable signals in their ^1H NMR spectra for both the *Pro-R* and *Pro-S* methylene protons. These protons experience geminal couplings ($^2J_{HH}$) ranging from 8.5 to 20 Hz upon loss of equivalency. The splitting patterns of the methylene resonances H(6) and H(7) as well as H(17) and H(18) in the Ga(III) complex show *AX*-quartets with large chemical shift separations, $\Delta\delta$. The signals for these protons are field dependent and the $\Delta\delta$ values are largest for the Co(III) complex, Figure 6. The signals for the protons of the diamine backbone, H(9) and H(11), appear as complex multiplets in the Co(III) and Ga(III) complexes due to the presence of both vicinal and geminal couplings. The resonances of the diamine backbone in the In(III)−$bppd^{2-}$ complex ion, however, are somewhat different. The pentuplet arising from H(10) is slightly broadened and a return to equivalency is observed for H(9a,b), which appears as a triplet.

Distinguishing between *trans*-O,O and *trans*-N_{py},N_{py} isomers in pseudo-octahedral $[M(bppd)]^+$ complexes, both of which display C_2 symmetry, can be achieved through the application of 2D NOESY experiments.[3] The spatial proximity of the definitive hydrogen atoms for the *trans*-O,O and *trans*-N_{py},N_{py} isomers of $[Co(bppd)]^+$ and $[In(bppd)]^+$ that are expected to give rise to unique NOE correlations are given in Table 6. These distances, which were used to identify anticipated NOE correlations, were determined using the atom coordinates of the energy minimized structures obtained from the ab initio Hartree−Fock HF/6-31G* calculations.

dx.doi.org/10.1021/ic402810e | *Inorg. Chem.* 2014, 53, 3404−3416

A unique NOE correlation exists between H(7a) of the acetate functionality and H(10) of the central carbon in the propylene backbone in the *trans*-O,O isomer because of their close proximity. This correlation is lacking in the *trans*-N_{py},N_{py} isomer because of the larger separation, Table 6. Similar unique NOE correlations exist between H(6) of a 2-pyridylmethyl group and H(10) of the propylene backbone, and H(1) of a 2-pyridylmethyl group and H(18) of the acetate group on the other amine nitrogen. Complexes displaying a *trans*-N_{py},N_{py} geometry would show these NOE correlations whereas a *trans*-O,O complex would not. Thus, it is these unique NOE correlations that can be used to definitively distinguish between *trans*-O,O and *trans*-N_{py},N_{py} $[M(bppd)]^+$ isomers.

The 2D NOESY spectrum for the *trans*-O,O $[Co(bppd)]^+$ complex (Figure S7) shows an off-diagonal peak arising from a NOE correlation between H(7a) and H(10), which are separated by 2.39 Å. NOE correlations between H(6)−H(10) and H(1)−H(18), separated by 4.38 and 5.95 Å, respectively, are not observed. The 2D NOESY spectrum of the $[In(bppd)]^+$ complex, Figure 7, which exhibits the smallest differences in calculated free energies for the 3 possible isomers, is similar to that of the $[Co(bppd)]^+$ complex. The observed unique correlation between H(7a) and H(10), which are in this case separated by 2.51 Å, is shown in green, while the correlation between H(6) and H(4), which is not unique is shown in purple. No NOE correlations are observed between H(6) and H(10) at 4.38 Å or H(1) and H(18) at 6.35 Å. Thus, the NMR data strongly suggest the presence of the *trans*-O,O $[In(bppd)]^+$ isomer similar to that observed for the $[Co(bppd)]^+$ cation, which is consistent with the calculated ΔG in solution values in Table 4.

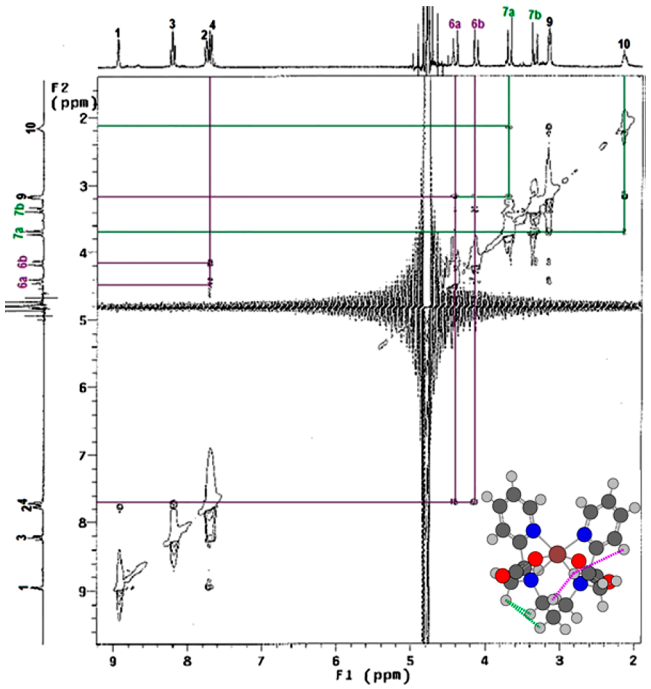

Figure 7. 2D NOESY plot for $[In(bppd)]^+$ showing NOE correlations for the methylene protons of the 2-pyridylmethyl group, H(6) (purple), and the acetate group, H(7) (green). The plot displays the ^{1}H NMR spectrum from 2.4−9.8 ppm on the *x* axis and from 2.2−9.3 ppm on the *y* axis.

The investigated Ln(III) complexes all give rise to 8 broadened resonances in the ^{1}H NMR spectrum and 10 resonances in the ^{13}C spectrum. The number of observed resonances indicates the presence of a single species displaying C_2 symmetry, while the broadened ^{1}H resonances signify the presence of a less rigid molecule.[46] The methylene protons assigned as H(6), H(7), and H(9) retain equivalency and appear as single resonances in the ^{1}H NMR spectrum, which is characteristic of an achiral environment. The broadened signals and observed equivalency in the methylene protons is suggestive of a Ln(III)−$bppd^{2-}$ interaction that is predominately ionic. These findings are consistent with the view that $bppd^{2-}$ adopts a nestlike structure when binding to Ln(III) ions and that the metal−ligand bonding is nondirectional.

The ^{1}H and ^{13}C NMR spectra for $[Al(bppd)]PF_6$ are very similar to those for $[La(bppd)]PF_6$, but without line broadening of the ^{1}H signals. The Al(III)−$bppd^{2-}$ complex gives 8 ^{1}H and 10 ^{13}C resonances characteristic of a species with C_2 symmetry. The quantum mechanical calculations for a distorted octahedral $[Al(bppd)]^+$ complex indicate that because of the steric repulsions between the pyridine rings all 3 possible isomers for a hexacoordinate $bppd^{2-}$ complex are considerably less energetically favorable than a hexacoordinate Al(III) complex in which the 2-pyridylmethyl groups are replaced by water, Figure 4. The *trans*-O,O $[Al(bppd)(H_2O)_2]^+$ structure, which is the energetically most favorable solution species, retains C_2 symmetry and removes the steric repulsion between the pyridine rings while allowing intramolecular hydrogen bonding with the coordinated H_2O molecules. The ^{1}H NMR spectrum shows 3 sharp singlets arising from the diastereotopic protons H(6), H(7), and H(9), which is either the result of rapid conformational interchange on the NMR time scale causing signal averaging or proton equivalency arising from a decrease in restricted motion about the diamine nitrogens.[47] In the diaqua complex, this latter effect would be enhanced by the increased mobility of the two uncoordinated 2-pyridylmethyl groups and most likely is responsible for the observed equivalency in the diastereotopic methylene proton signals.

CONCLUSIONS

Different types of carboxylate binding modes were determined from the separation between antisymmetric and symmetric COO^- stretching frequencies, $\Delta\nu = \nu_a(COO^-) - \nu_s(COO^-)$, in $[M(bppd)]^+$ complexes. The acetate groups in the Al(III), Ga(III), In(III), and Co(III), metal-$bppd^{2-}$ complexes are bound in a monodentate fashion whereas the binding in the $[Ln(bppd)]^+$ complexes is ionic. *cis*-O,O; *cis*-N_{py},N_{py} (C_1 symmetry) and *trans*-O,O (C_2 symmetry) isomers for pseudo-octahedral metal-$bppd^{2-}$ complexes were observed in the solid state for Ga(III) and Co(III), respectively. The third and least stable possible $[M(bppd)]^+$ isomer with *trans*-N_{py},N_{py} pyridine groups was not observed for any metal ion investigated. Classical ^{1}H and ^{13}C NMR spectroscopy differentiated and confirmed that the conformations observed in the solid state are also the dominate species in aqueous solution. The 2D NOESY experiments were used to discriminate between the *trans*-O,O and *trans*-N_{py},N_{py} isomers of the $[Co(bppd)]^+$ and $[In(bppd)]^+$ complexes. Quantum mechanical calculations were used to gain insight into the relative stability of the geometric isomers and the type of metal−ligand bonding as well as changes in ligand denticity ($[Al(bppd)]^+$) and metal coordination numbers ($[Ln(bppd)(H_2O)_2]^+$).

dx.doi.org/10.1021/ic402810e | *Inorg. Chem.* 2014, 53, 3404−3416

■ ASSOCIATED CONTENT

Supporting Information

Structural details for [Ga(bppd)]PF_6, ^{13}C NMR spectral data for H_2bppd and $[M(bppd)]^+$ complexes, IR spectra for cis-[Ga(bppd)]PF_6 and *trans*-[Co(bppd)]PF_6, 2D COSY, NOESY, and HSQC plots for *cis*-O,O; *cis*-N_{py},N_{py} [Ga(bppd)]PF_6, and 2D NOESY and HSQC plots for *trans*-O,O [Co(bppd)]PF_6. This material is available free of charge via the Internet at http://pubs.acs.org.

■ AUTHOR INFORMATION

Corresponding Author

*E-mail: aherlin@luc.edu.

Notes

The authors declare no competing financial interest.

■ ACKNOWLEDGMENTS

This work was supported by Illinois State University, Loyola University Chicago, and the National Science Foundation (US, CHE-0645081). CCM acknowledges the National Science Foundation for the purchase of the Bruker APEXII (CHE-10−39689). DSK wishes to thank Loyola University Chicago and the Schmitt Foundation for fifth year fellowship support. We thank Professor M. Paul Chiarelli for the kind use of his mass spectrometer facilities and Ms. Qian Wang for recording the mass spectra data. We also thank Dr. Yuyang Wu of Northwestern University for recording the $^1H-^{13}C$-detected HSQC NMR spectra.

■ REFERENCES

(1) Choppin, G. R.; Thakur, J. N.; Mathur, J. N. *Coord. Chem. Rev.* **2006**, *250*, 936−947 and references therein.

(2) Weaver, B.; Kappelmann, F. A. *Oak Ridge National Laboratory Report to the U.S. Atomic Energy Commission*; Oak Ridge National Laboratory: Oak Ridge, TN, 1964, pp 1−61.

(3) Caravan, P.; Rettig, S. J.; Orvig, C. *Inorg. Chem.* **1997**, *36*, 1306−1315.

(4) Caravan, P.; Mehrkhodavandi, P.; Orvig, C. *Inorg. Chem.* **1997**, *36*, 1316−1321.

(5) Geraldes, C. F. G. C. *NMR Supramol. Chem.* **1999**, *526*, 133−154.

(6) Heitzmann, M.; Bravard, F.; Gateau, C.; Boubals, N.; Berthon, C.; Pecaut, J.; Charbonnel, M. C.; Delangle, P. *Inorg. Chem.* **2009**, *48*, 246−256.

(7) Weiner, R. E.; Thakur, M. L. *Radiochim. Acta.* **1995**, *70*, 273−287.

(8) Jensen, M. P. *J. Alloys Compd.* **2000**, *303*−*304*, 137−145.

(9) Ogden, M. D.; Meier, G. P.; Nash, K. L. *J. Solution Chem.* **2012**, *41*, 1−16.

(10) Hancock, R. D. *Pure Appl. Chem.* **1986**, *58*, 1445−1452.

(11) Hancock, R. D. *Acc. Chem. Res.* **1990**, *23*, 253−257.

(12) Cukrowski, I.; Cukrowska, E.; Hancock, R. D.; Anderegg, G. *Anal. Chim. Acta* **1995**, *312*, 307−321.

(13) Hancock, R. D.; Martell, A. E. *Chem. Rev.* **1989**, *89*, 1875−1914.

(14) Kanamori, K.; Kyotoh, A.; Fujimoto, K.; Nagata, K.; Suzuki, H.; Okamoto, K. *Bull. Chem. Soc. Jpn.* **2001**, *74*, 2113−2118.

(15) Lacoste, R. G.; Christoffers, G. V.; Martell, A. E. *J. Am. Chem. Soc.* **1965**, *87*, 2385−2388.

(16) Mandel, J. B.; Maricondi, C.; Douglas, B. E. *Inorg. Chem.* **1988**, *27*, 2990−2996.

(17) Mandel, J. B.; Douglas, B. E. *Inorg. Chim. Acta* **1989**, *155*, 55−69.

(18) Kanamori, K.; Matsui, N.; Takagi, K.; Miyashita, Y.; Okamoto, K. *Bull. Chem. Soc. Jpn.* **2006**, *79*, 1881−1888.

(19) Sato, K.; Ohnuki, T.; Takahashi, H.; Miyashita, Y.; Nozaki, K.; Kanamori, K. *Inorg. Chem.* **2012**, *51*, 5026−2036.

(20) Zhang, Q.; Gorden, J. D.; Beyers, R. J.; Goldsmith, C. R. *Inorg. Chem.* **2011**, *50*, 9365−9373.

(21) McLauchlan, C. C.; Kissel, D. S.; Arnold, W.; Herlinger, A. W. *Acta Crystallogr.* **2013**, *E69* (5), m296−m297.

(22) Gottlieb, H. E.; Kotlyar, V.; Nudelman, A. J. *J. Org. Chem.* **1997**, *62*, 7512−7515.

(23) Bruker. *APEX2*, *SAINT*, and *SADABS*; Bruker AXS Inc.: Madison, WI, U.S.A., 2008.

(24) Sheldrick, G. M. *Acta Crystallogr.* **2008**, *A64*, 112−122.

(25) Hehre, W. J.; Radom, L.; Schleyer, P. V. R.; Pople, J. *Molecular Orbital Theory*; Wiley-Interscience: New York, 1986.

(26) Igel-Mann, G.; Stoll, H.; Preuss, H. *Mol. Phys.* **1988**, *65*, 1321−1328.

(27) Kuechle, W.; Dolg, M.; Stoll, H.; Preuss, H. *Mol. Phys.* **1991**, *74*, 1245−1263.

(28) Dolg, M.; Stoll, H.; Preuss, H. *Theor. Chem. Acc.* **1993**, *85*, 441−450.

(29) Cao, Y.; Dolg, M. *J. Chem. Phys.* **2001**, *115*, 7348−7355.

(30) Mennucci, B.; Cances, E.; Tomasi, J. *J. Phys. Chem. B.* **1997**, *101*, 10506−10517.

(31) Frisch, M. J.; Trucks, G. W.; Schlegel, H. B.; Scuseria, G. E.; Robb, M. A.; Cheeseman, J. R.; Montgomery, J. A., Jr.; Vreven, T.; Kudin, K. N.; Burant, J. C.; Millam, J. M.; Iyengar, S. S.; Tomasi, J.; Barone, V.; Mennucci, B.; Cossi, M.; Scalmani, G.; Rega, N.; Petersson, G. A.; Nakatsuji, H.; Hada, M.; Ehara, M.; Toyota, K.; Fukuda, R.; Hasegawa, J.; Ishida, M.; Nakajima, T.; Honda, Y.; Kitao, O.; Nakai, H.; Klene, M.; Li, X.; Knox, J. E.; Hratchian, H. P.; Cross, J. B.; Bakken, V.; Adamo, C.; Jaramillo, J.; Gomperts, R.; Stratmann, R. E.; Yazyev, O.; Austin, A. J.; Cammi, R.; Pomelli, C.; Ochterski, J. W.; Ayala, P. Y.; Morokuma, K.; Voth, G. A.; Salvador, P.; Dannenberg, J. J.; Zakrzewski, V. G.; Dapprich, S.; Daniels, A. D.; Strain, M. C.; Farkas, O.; Malick, D. K.; Rabuck, A. D.; Raghavachari, K.; Foresman, J. B.; Ortiz, J. V.; Cui, Q.; Baboul, A. G.; Clifford, S.; Cioslowski, J.; Stefanov, B. B.; Liu, G.; Liashenko, A.; Piskorz, P.; Komaromi, I.; Martin, R. L.; Fox, D. J.; Keith, T.; Al-Laham, M. A.; Peng, C. Y.; Nanayakkara, A.; Challacombe, M.; Gill, P. M. W.; Johnson, B.; Chen, W.; Wong, M. W.; Gonzalez, C.; Pople, J. A. *Gaussian 03*, revision C.02; Gaussian, Inc.: Wallingford, CT, 2004.

(32) Socrates, G. *Infrared Characteristic Group Frequencies*, 2nd ed.; John Wiley & Sons: New York, 1994.

(33) Ben-Naim, A. *J. Phys. Chem.* **1978**, *82*, 792−803.

(34) Strajbl, M.; Florián, J.; Warshel, A. *J. Phys. Chem. B.* **2001**, *105*, 4471−4484.

(35) Rotzinger, F. P. *J. Phys. Chem. B.* **2005**, *109*, 1510−1527.

(36) Allen, F. H. *Acta Crystallogr., Sect. B* **2002**, *58*, 380−388.

(37) Mulla, F.; Marsicano, F.; Nakani, B. S.; Hancock, R. D. *Inorg. Chem.* **1985**, *24*, 3076−3080.

(38) Herlinger, A. W.; Wenhold, S. L.; Long, T. V. *J. Am. Chem. Soc.* **1970**, *92*, 6474−6480.

(39) Nakamoto, K. *Infrared Spectra of Inorganic and Coordination Compounds*, 4th ed.; John Wiley & Sons: New York, 1986.

(40) Deacon, G. B.; Phillips, R. J. *Coord. Chem. Rev.* **1980**, *33*, 227−250.

(41) Curtis, N. F. *J. Chem. Soc. (A)* **1968**, 1579−1584.

(42) Mather, D. J.; Tapscott, R. E. *J. Coord. Chem.* **1981**, *11*, 5−10.

(43) Parker, D.; Waldron, P.; Yufit, D. S. *Dalton Trans.* **2013**, *42*, 8001−8008.

(44) Buddhadev, S.; White, G. L.; Wander, J. D. *J. Chem. Soc., Dalton Trans.* **1972**, *4*, 447−449.

(45) Anet, F. A. L.; Kopelevich, M. *J. Am. Chem. Soc.* **1989**, *111*, 3429−3431.

(46) Platas, C.; Avecilla, F.; de Blas, A.; Geraldes, C. F. C. G.; Rodriquez-Blas, T.; Adams, H.; Mahia, J. *Inorg. Chem.* **1999**, *38*, 3190−3199.

(47) Shvo, Y.; Taylor, E. C.; Mislow, K.; Raban, M. *J. Am. Chem. Soc.* **1967**, *89*, 4910−4917.